Conceptual design of an aircraft for Mars mission

Abstract

Purpose – The purpose of this paper is to present the results of a conceptual design of Martian aircraft. This study focuses on the aerodynamic and longitudinal dynamic stability analysis. The main research questions are: does a tailless aircraft configuration can be used for Martian aircraft? How to the short period characteristic can be improved by side plates modification?

Design/methodology/approach – Due to a conceptual design stage of this Martian aircraft, aerodynamic characterises were computed by the Panukl package which using the potential flow model. The longitudinal dynamic stability was computed by Matlab code, the derivatives computed by the SDSA software were used as the input data. Different aircraft configurations have been studied, including different wing's aerofoils, and configurations of the side plate.

Findings – This paper presenting results aerodynamic characteristics computations and longitudinal dynamic stability analysis. This paper shows that tailless aircraft configuration has potential to be used as Martian aircraft. Moreover, the study of the impact of side plates' configurations on the longitudinal dynamic stability is presented. This investigation reveals that the most effective method to improve the short period damping ratio is change the height of the bottom plate.

Practical implications – The presented result might be useful in case of a further design of the aircrafts for the Mars mission and designing the aircrafts in a tailless configuration.

Social implications – Mars is the most probability planet to explore by the human expedition. This paper presents the conceptual study into aircraft which can be used to taking the high-resolution pictures of the surface of Mars, which can be crucial to find the right place to establish a potential Martian base.

Originality/value – Most of aircrafts proposed for the Mars mission are designed in a configuration with a classic tail, this paper shows a preliminary calculation of the tailless Martian aircraft. Moreover, this paper shows the results of a dynamic stability analysis, where similar papers about aircrafts for the Mars mission do not show such outcomes, especially in the case of the tailless configuration. Moreover, this paper presents the results of the dynamic stability analysis of tailless aircraft with different configurations of the side plates.

Keywords Aircraft for Mars mission, stability analysis, CFD.

Paper type *Research paper*

Introduction

So far, Mars exploration has been done using orbiters, landers, and rovers. However, rovers' range is restricted, therefore only the area close to a landing point can be photographing by rovers. On the other hand, orbiters observe Mars from orbits, which are far from the surface. In 2018, NASA launched on the Atlas V 401 rocket the InSight project. This mission's payload includes not only the lander but also two 6U CubeSats, which is the first attempt to use a CubeSat in a deep space [NASA webs site]. In case of a more extensive Mars exploration, including a preparation for the first manned mission, collecting more information about a potential place for a Martian base is required. A small UAV could fly close to the ground surface and collect high-resolution pictures. An example of a project which is developing a rocket for a human Mars mission is SpaceX BFR project.

A few projects of aircraft for Mars are been developing but none of those designs have been launched on Mars yet. A few different concepts have been investigating, for example the NASA project [Guynn et l (2003)] for ARES mission; a solar aircraft [Noth et al (2004)] as well as rotorcraft [Young at al (2005)]. Moreover, the study into Martian aircraft aerodynamic [Anyoji et al (2017), Naoya Fujioka et al (2014)] is also conducted. All listed aircraft concepts are assuming designing the aircraft in classic configuration. This paper presents the results of the conceptual design of Martian aircraft in a tailless configuration. The presented aircraft concept can be used as a platform for Martian surface photographing.

Mars Atmosphere

The Martian atmosphere has a lower density than the atmosphere of Earth, the density at the altitude close to Mars ground surface corresponds to the density of the atmosphere of Earth at the altitude of 33 kilometres. On the other hand, the gravity acceleration on Mars is lower than on Earth and is equal to 3.8 m/s^2. Figure 1 presents the lift coefficient of Martian aircraft versus true airspeed; those results have been plotted for different altitudes. The presented data was calculated for the aircraft mass equal to 6.0 kilograms and wing area equal to 0.906m^2. Figure 2 presents Reynolds number and Mach number versus true airspeed; those results correspond to flying on the altitude equal to 2.17 kilometres. A speed of the sound on Mars is lower than on Earth and is equal to 230 m/s, which means that the compressible effect occurs for a lower speed than on Earth. The Reynolds number is lower than the typical values used in case of an aircraft design for flights in the atmosphere of Earth. Moreover, properties of the atmosphere of Mars are not uniform and might depend on a longitude and latitude. In this paper, the Mars Global Reference Atmospheric Model 2005 was used in all calculations, this model is presented in [Justus, Johnson (2001),]. The Martian atmosphere has also a different air composition and consists of 0.13% of oxygen only, therefore the best type of engine will be the rocket engine.

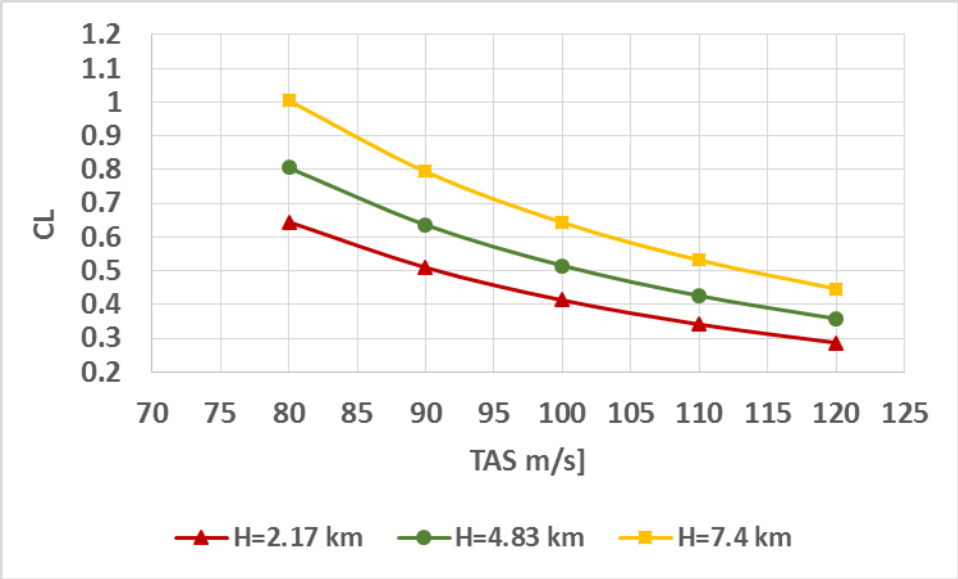

Figure 1 Lift coefficient versus true airspeed for different altitudes

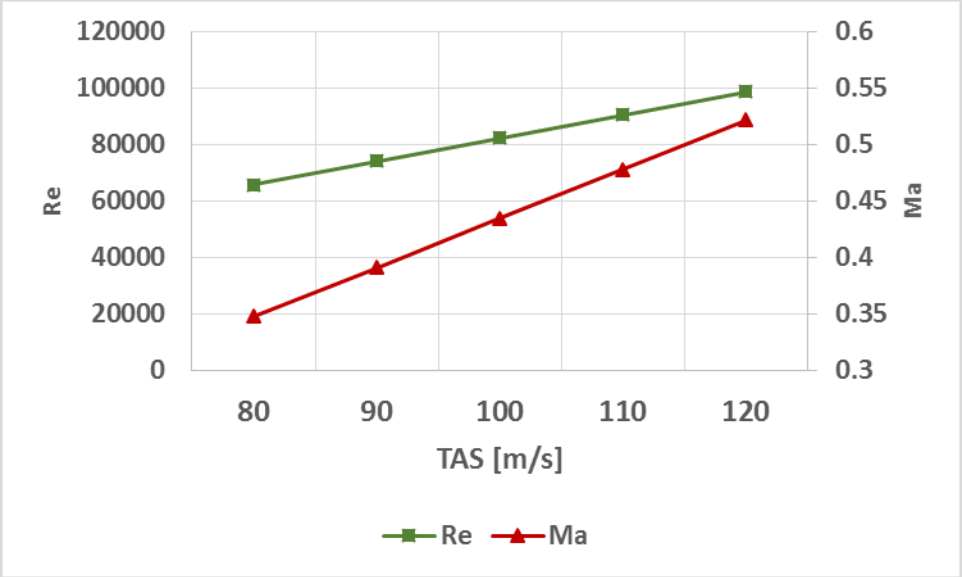

Figure 2 Reynolds and Mach number versus true airspeed in case of Martian aircraft flying at 2.17 km.

Mission Definition

According to the mission assumptions, the Martian aircraft can be transporting on Mars using the Atlas V rocket. The weight of aircraft's payload is about 1 kilogram, the cruising speed range is 110-120 m/s, and the maximum weight of the aircraft should be less than 6.5 kg. Due to the air composition of the atmosphere of Mars, the aircraft will be equipped with the rocket engine.

Aircraft Geometry

The tailless configuration was selected for this Martian aircraft. Such a configuration is more compact compared to a configuration with a classic tail, therefore the aircraft does not require to be foldable during the transportation between Earth and Mars. The delta wing was selected as a wing platform, such configuration can be useful if aircraft would be dropped during the atmosphere entry, because the delta wing can generate a lift vortex which can be used to decrease a sink rate, moreover, the delta wing is good in terms of flying in stall conditions [Figat et al (2012), Galiński at el (2007)]. The pitch channel will be controlled by elevons or by rotating all moving plates (in unsymmetrical deflection) [Figat et al (2012), Galiński at el (2007), Kwiek and Figat (2016)]. The elevons cover 30% of a local chord, and the span of elevons covers 20% to 89% of the wingspan. The roll channel will be controlled by elevons and the yaw channel will be controlled by rotating of all moving plates (in symmetrical deflection). A few different configurations of the aircraft were investigated, the basic geometrical data is presented in Table 1. Figure 3 shows the definition of the side plates geometrical parameters. Figure 4 is presenting the layout of one of the analysed configurations of the aircraft - model v7.

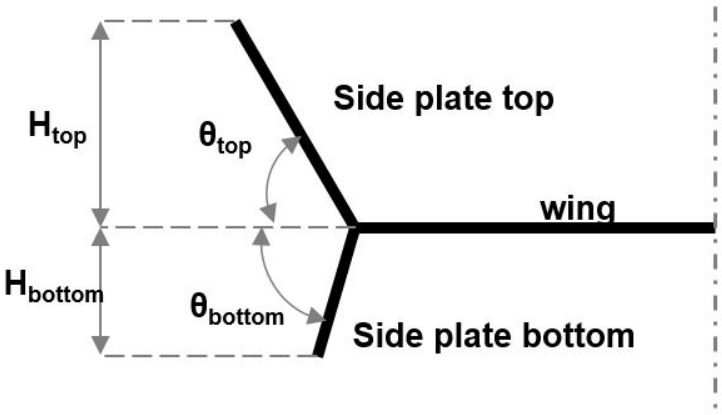

Figure 3 Definition of the side plate geometrical parameters

Table 1 Martian aircraft geometrical parameters

Parameters	Model v1,2,3	Model v4,5	Model v6	Model v7,8,9	Model v10,11
Wing area [m^2]	0.906	0.906	0.906	0.906	0.906
Wing Span [m]	1	1	1	1	1
Aerofoil	A18 A18/CJ6 A18/E374	A18/CJ6 A18/E374	A18/CJ6	A18/CJ6 A18/E374 A18	A18/CJ6 A18
H_{top} [m]	0.2	0.25	0.25	0.25	0.25
H_{bottom} [m]	0.12	0.18	0.18	0.15	0.12
θt_{op} [deg.]	63.43	59	59	59	59
θ_{bottom} [deg.]	90	65	90	90	90

Span with tail plates [m]	1.2	1.3	1.3	1.3	1.3
MAC [m]	0.957	0.957	0.957	0.957	0.957
XCG [%MAC]	27.64%	27.38%	27.38%	33.41%	33.26%
Iy [kg*m^2]	0.614	0.654	0.655	0.643	0.636
Mass [kg]	6	6.16	6.16	6.11	6.09

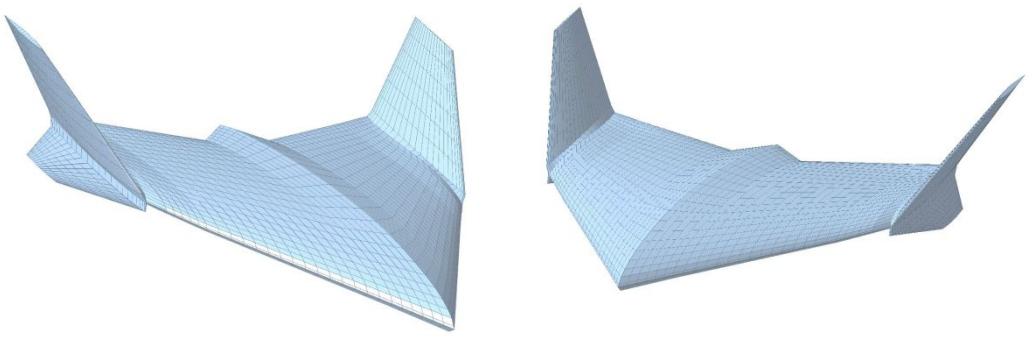

Figure 4 Geometry of the Martian aircraft

Aerodynamic characteristics

This paper presents only a preliminary investigation into the Martian aircraft. Due to the preliminary stage of the design, the aerodynamic characteristics were computed by Panukl package (Panukl 2018). This software using a low order potential method, moreover, the impact of compressible effect was included by Karman-Tsien correction. Due to the very low Reynolds number when the viscosity effect is significant the Panukl drag coefficient results were modified by using the empirical equation for a friction drag estimation. The aerodynamic forces and moment coefficients are presented in Figure 5-7 because the data was computed by the panel method only a linear part of the lift coefficient was taken into consideration.

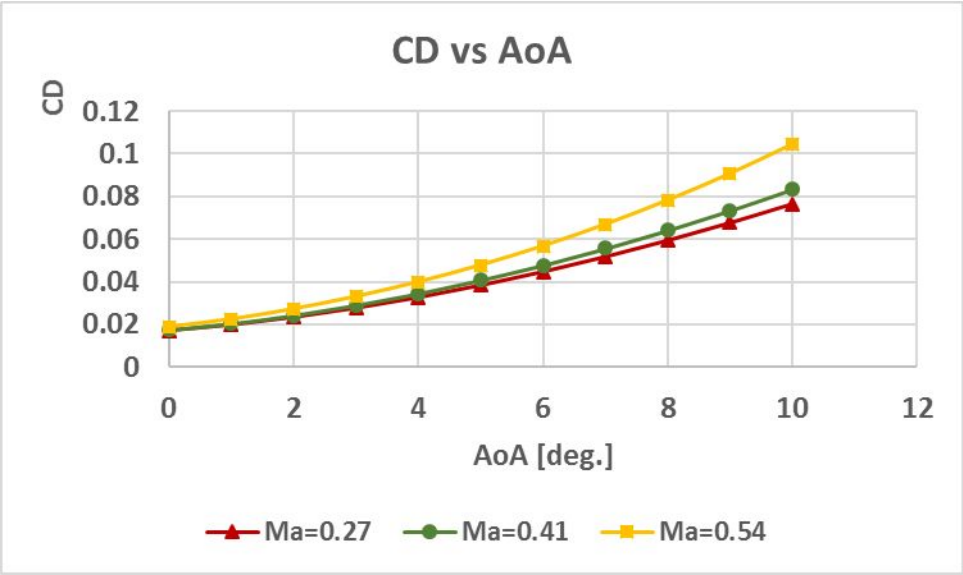

Figure 5 Drag coefficient versus angle of attack, model v11

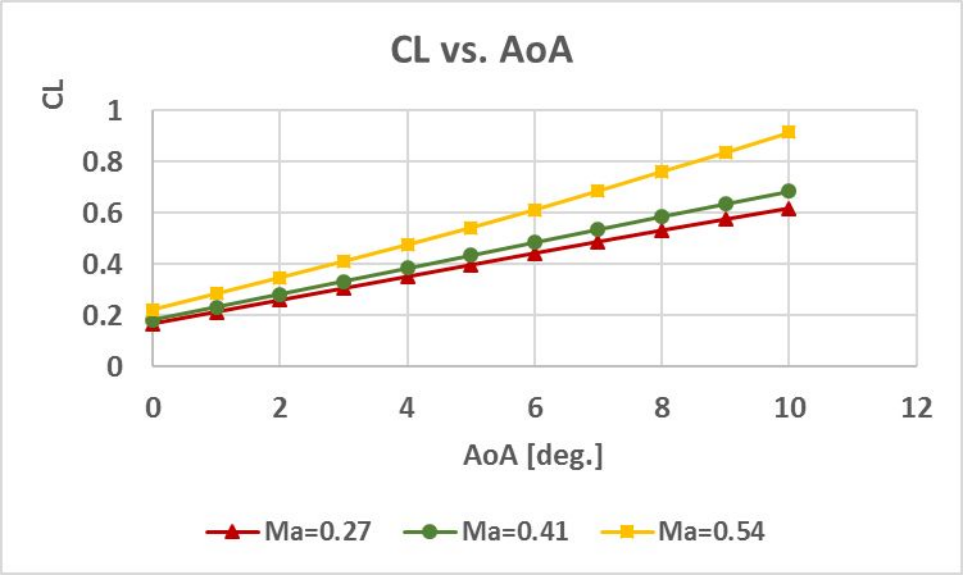

Figure 6 Lift coefficient versus angle of attack, model v11

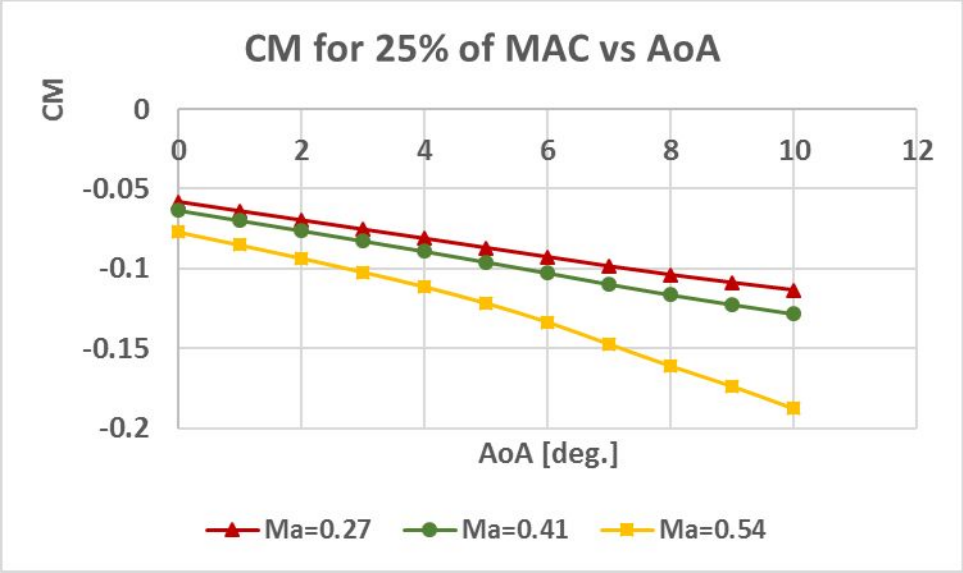

Figure 7 Pitching moment coefficient for the reference point of 25% of MAC versus angle of attack, model v11

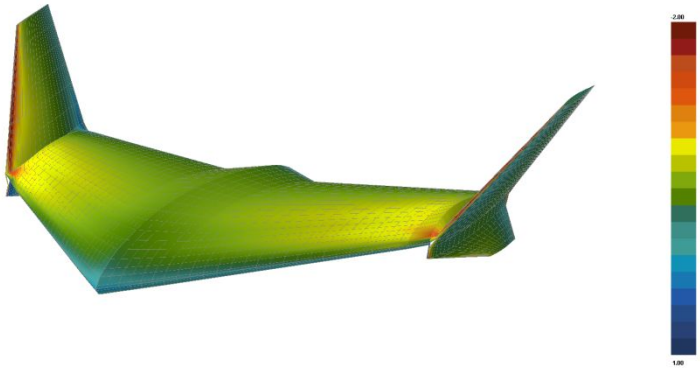

Figure 8 Pressure distribution for model v11 and AoA=5deg., Ma=0.41

Longitudinal Stability

Static stability

The dynamic stability was computed by SDSA package [Goetzendorf-Grabowski et al (2011), SDSA (2018)] based on the Panukl package results. Figure 9 presents the static stability margin versus angle of attack for the case of model v1 and model v11. The aircraft is statically stable for the whole analysed range of angles of attack.

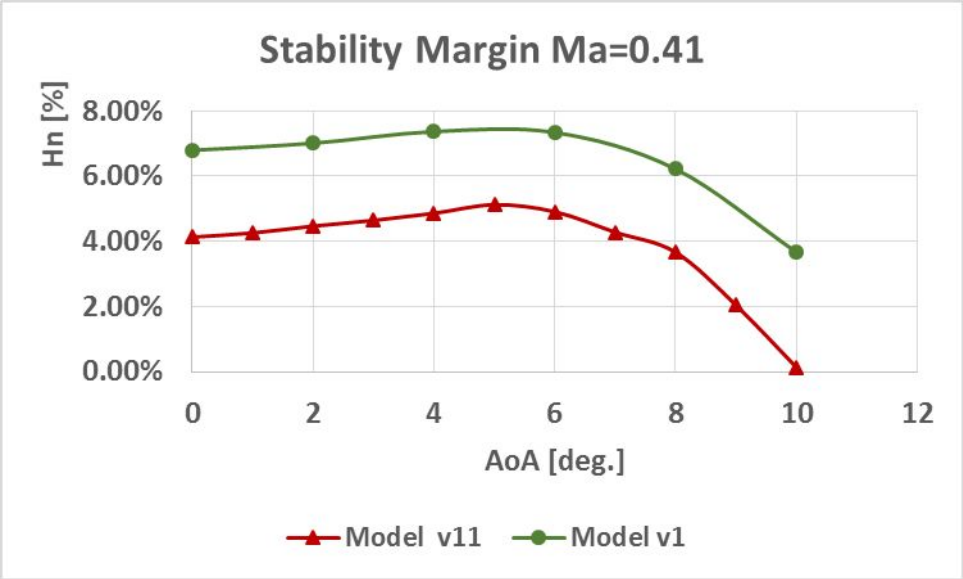

Figure 9 Aircraft static stability margin in case of the model v1 and v11 for Ma=0.41

Dynamic stability

The most popular way to solve equations of motion is linearization around the trim point using stability derivatives, this approach is described in the literature [Cook, (2007), Etkin, and Reid (1996), Nelson (1998)]. The dynamic stability was computed by SDSA software and Matlab code. The SDSA software was used for the stability derivatives calculation [Cook, (2007), Etkin, and Reid (1996)]. The Matlab code was used to solve the aircraft equation of motion in a state space form, which can be expressed by equations (1)-(4) [Cook, (2007)]; those equations presenting only the longitudinal model of the dynamic stability with assumption that equations of motion can be decoupling [Cook, (2007)]. The Matlab code solves the eigenvalue problem described by equations (5)-(6) and the solution is expressed by equation (7). A damping ratio, undamped frequency, period, and halftime to damping can be expressed by equations (8)-(11) respectively.

$$\dot{x} = Ax + Bc \quad (1)$$

$$x = [u \quad w \quad q \quad \theta]^T \quad (2)$$

$$A = M^{-1}A' \quad (3)$$

$$A = \begin{bmatrix} xu & xw & xq & x\theta \\ zu & zw & zq & z\theta \\ mu & mw & mq & m\theta \\ 0 & 0 & 1 & 0 \end{bmatrix} \quad (4)$$

$$x(t) = x_0 e^{\lambda t} \quad (5)$$

$$(A - \lambda I)x_0 = 0 \quad (6)$$

$$\lambda = \xi + i\eta \quad (7)$$

$$\zeta_d = -\frac{\xi}{\sqrt{\xi^2+\eta^2}} \quad (8)$$

$$\omega_{nd} = \sqrt{\xi^2 + \eta^2} \quad (9)$$

$$T = \frac{2\pi}{\eta} \quad (10)$$

$$T_{1/2} = -\frac{\ln 2}{\xi} \quad (11)$$

The trim conditions were computed by SDSA, this software has only data about the atmosphere of Earth. The trim calculations were done at the altitude equal to 33900m, this condition corresponds to the Martian air density at 2.17 kilometres. Due to a different gravity acceleration, the mass of the aircraft in SDSA was decreased to simulate the condition on Mars, the results are presented in Figure 10.

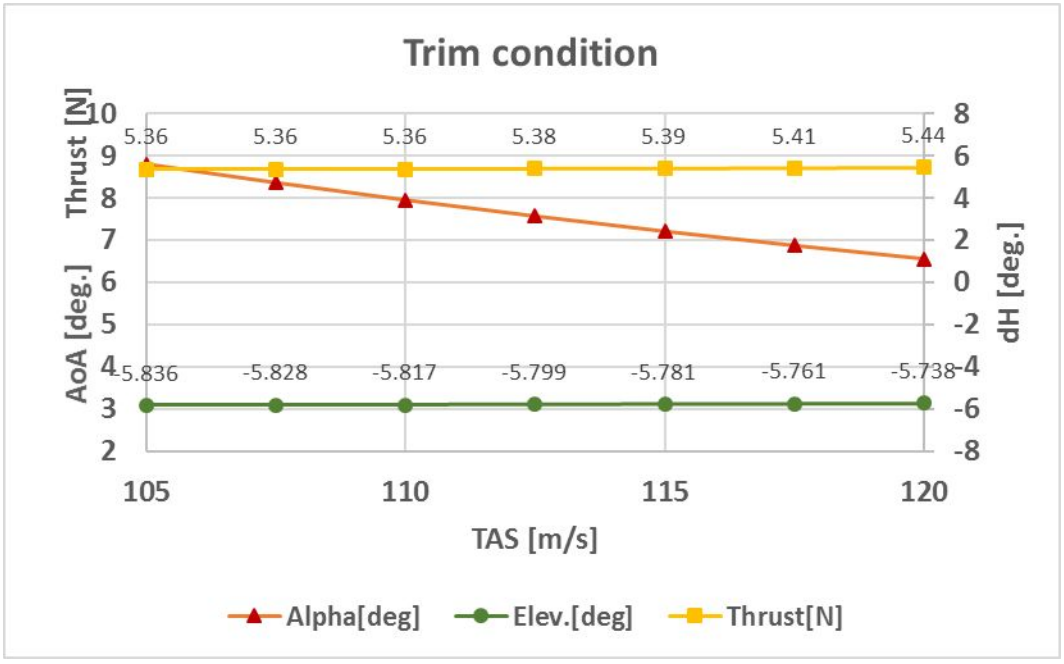

Figure 10 Trim condition – model v11

The results of the dynamic stability were computed by the Matlab based on the trim conditions and derivatives computed by the SDSA. This research focuses on the dynamic stability analysis of different configurations of the aircraft. Firstly, different wing's aerofoils were tested A18 (model v1), A18 & CJ6 (model v2), and A18 & E374 (model v3). The results of

the short period and phugoid computations are presented in Figure 11 and Figure 12. The aircraft is damping the longitudinal oscillation for the whole range of the speed. However, according to MIL-F-8785C regulation, to achieve level 3 of the dynamic stability, the damping ratio of the short period should be at least 0.15. Figure 11 shows that the strongest damping ratio occurs for the model v1, but all the presented models achieve the damping ratio smaller than 0.15.

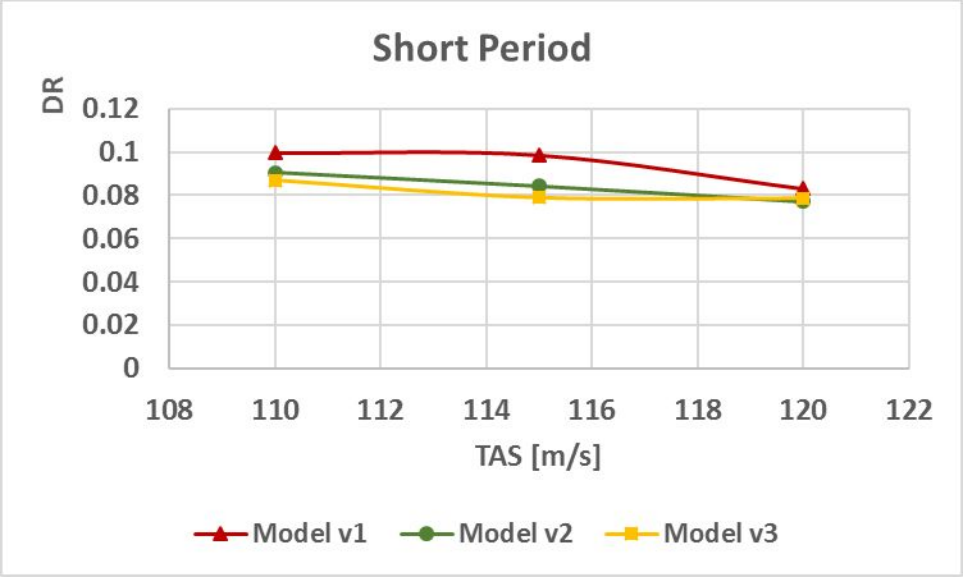

Figure 11 Damping ratio of the short period mode, the same tail configuration but different aerofoil.

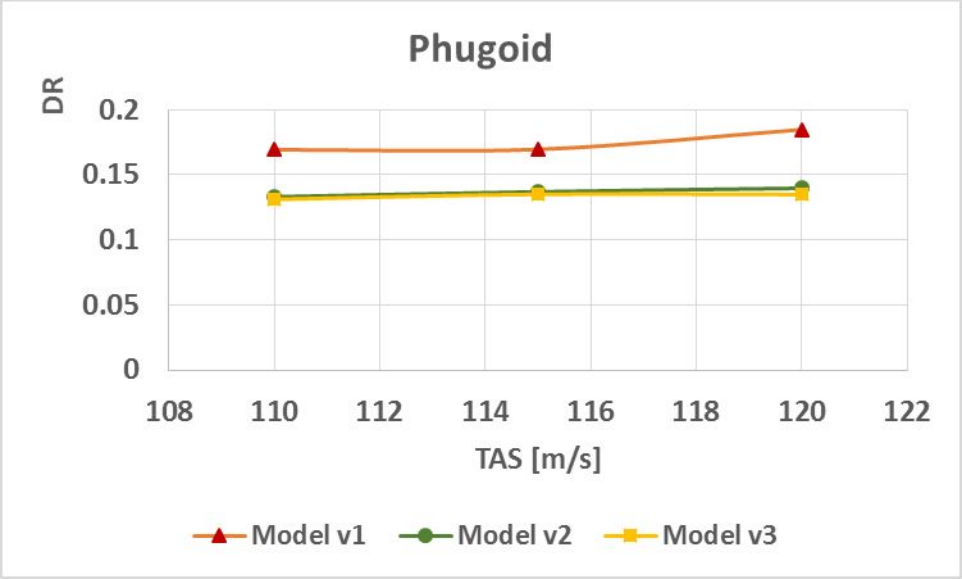

Figure 12 Damping ratio for the phugoid mode, the same tail configuration but different aerofoil.

The next geometrical parameter which was investigated is the angle of the bottom plate. Figure 13 and Figure 14 present the damping ratio for the short period and phugoid mode of model v4 and model v6. The aircraft in configuration v6 (θ_{bottom} =90 deg.) has a stronger damping ratio for the short period, but still, according to MIL-F-8785C regulation, the damping

ratio is too small. In terms of phugoid mode, the model v4 (θ_{bottom}=65 deg.) has a stronger damping ratio, according to MIL-F-8785C regulation, both models of the aircraft are stable.

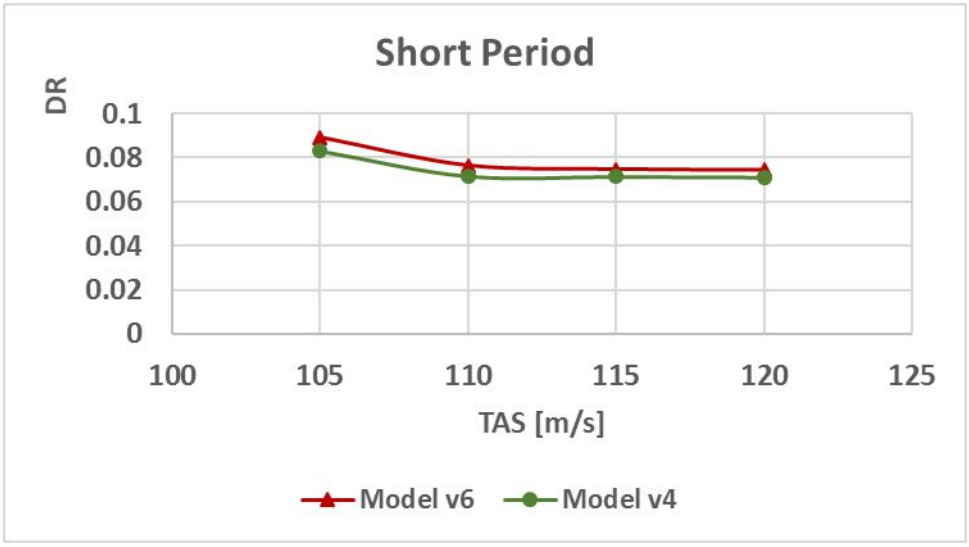

Figure 13 Damping ratio for the short period mode, the same size of side plates but different θ_{bottom}

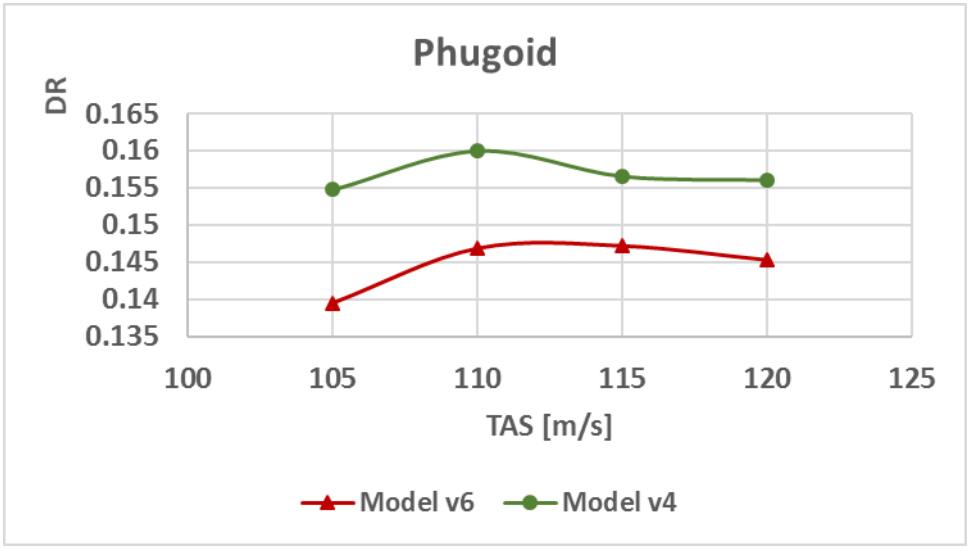

Figure 14 Damping ratio for the phugoid mode, the same size of side plates but different θ_{bottom}

The last investigated parameter was the height of the bottom plate, Figure 15 and Figure 16 show results for model v9 and model v11. In terms of the short period, the model v11 (with the smaller height) has damping ratio bigger than 0.15 for low speed (about 105 m/s), moreover, this damping ratio is stronger than the damping ratio of model v4. The phugoid damping ratios are very similar for both models and fulfil the MIL-F-8785C regulation.

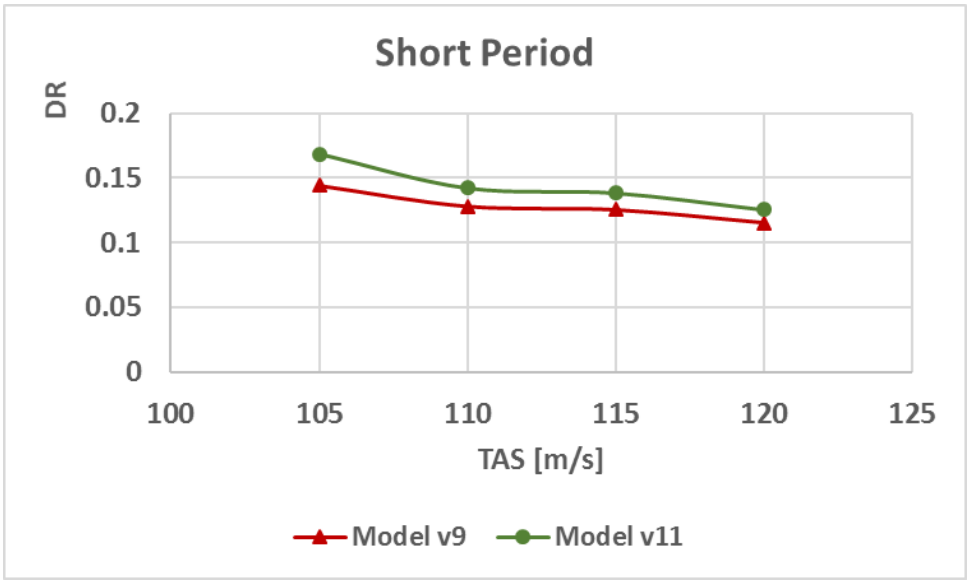

Figure 15 Damping ratio for the short period mode, the same size of side plates but different H_{bottom}

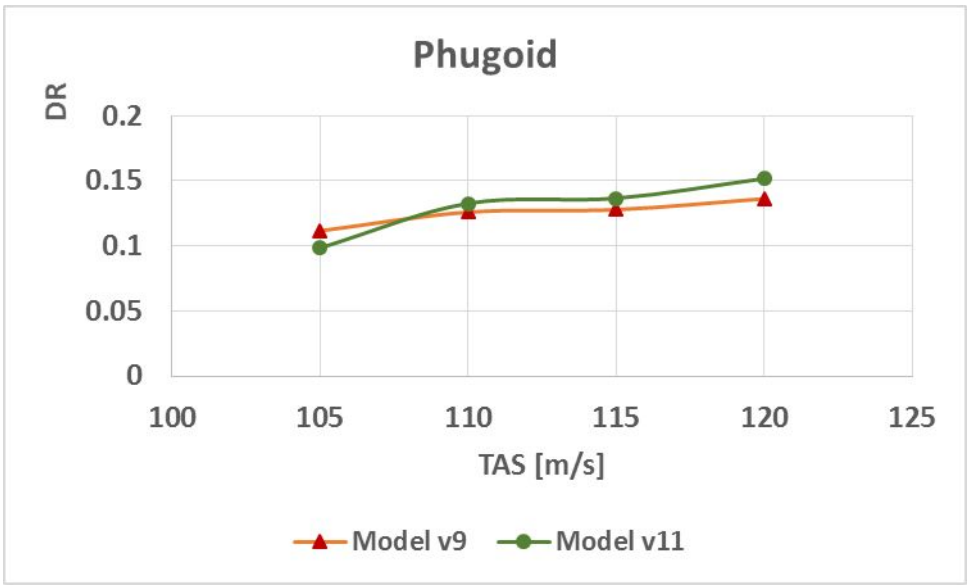

Figure 16 Damping ratio for the phugoid mode, the same size of side plates but different H_{bottom}

According to MIL-F-8785C regulation, the phugoid mode is stable for all considered models; the damping ratios classified the results for level 1. In case of the short period, according to MIL-F-8785C regulation, only model v11 is stable but only for low airspeed. The damping ratio of the rest of the analysed model is lower than 0.15. The most effective way to improve the short period damping ratio is changing the height of the bottom plate, this effect is not only related to the aerodynamic characteristics but also to the position of the CG and to the moment of inertia. In further analysis, the short period characteristics need to be improved. Model v11 complete results of the longitudinal dynamic stability are presented in Figure 17- Figure 20.

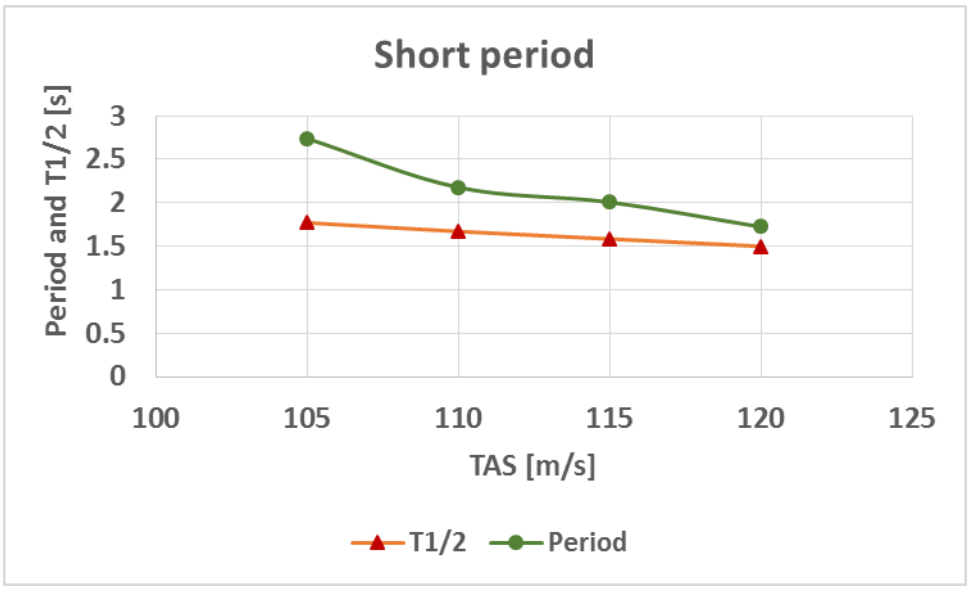

Figure 17 Results of the period and time to half damping for the short period mode, model v11

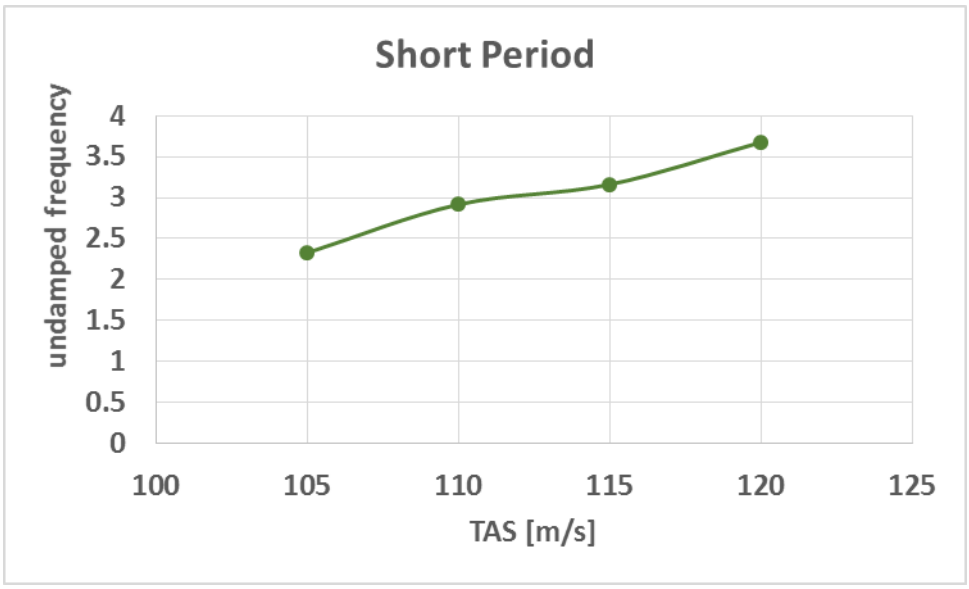

Figure 18 Results of the undamped frequency for the short period mode, model v11

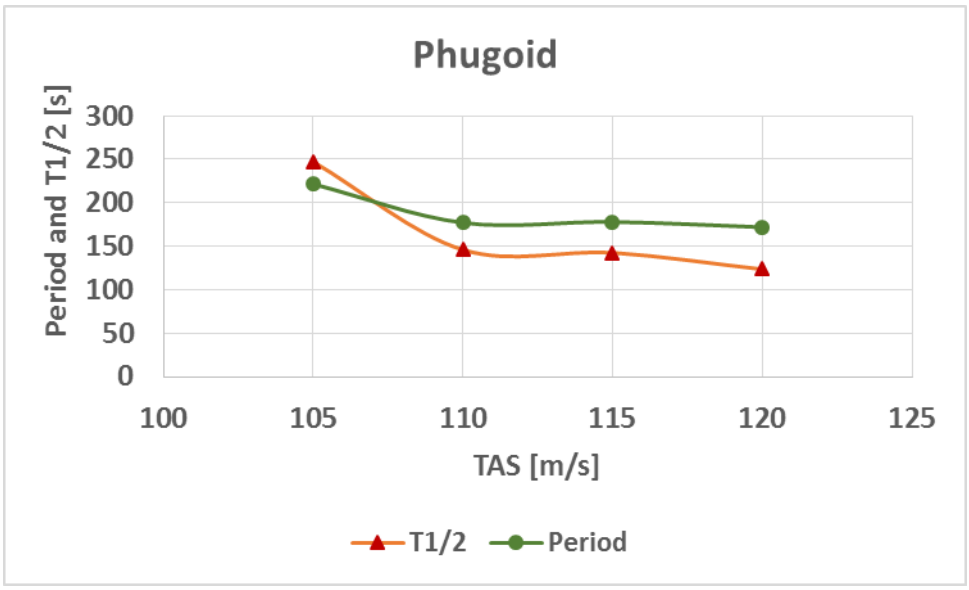

Figure 19 Results of the period and time to half damping for the phugoid mode, model v11

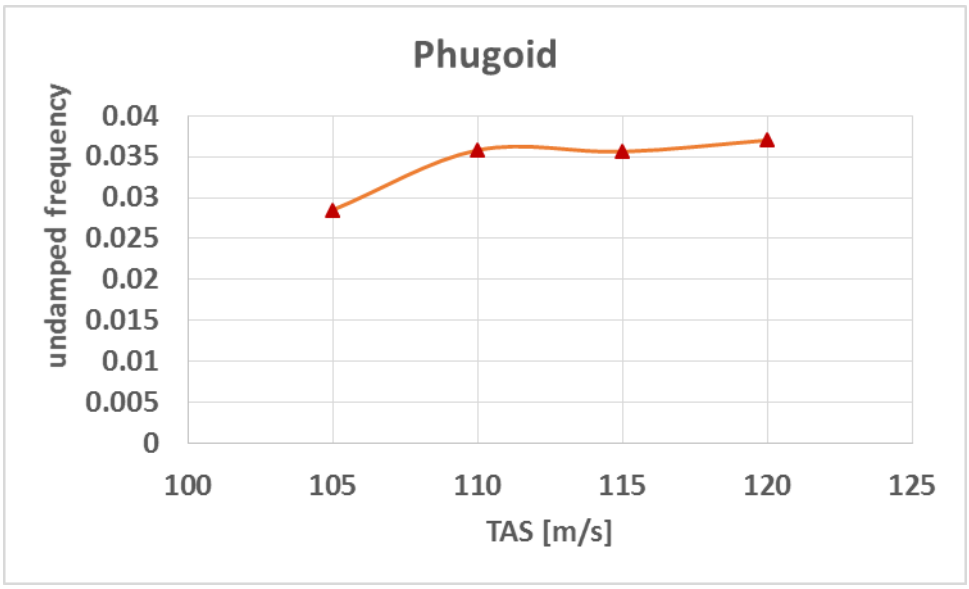

Figure 20 Results of the undamped frequency for the phugoid mode, model v11

Conclusion

Preliminary results of the aerodynamic analysis and dynamic stability analysis were presented. Due to a low density of the atmosphere of Mars, it is challenging to design the aircraft, but it is possible. However, it is recommended that aircraft fly with high speed due to the problem with a low Reynolds number. A few different configurations of the aircraft were analysed, including different aerofoils, the angle of the side plate, and the height of the bottom plate. All presented models have been designed in the tailless configuration, and all fulfil the MIL-F-8785C criteria for the phugoid mode, however, the short period mode required improvements. Only for the model v11 the short period damping ratio is bigger than 0.15. This

investigation reveals that the most effective method to improve this damping ratio was changing the height of the bottom plate.

Based on the presented results can be concluded that tailless aircraft has the potential to be the Martian aircraft, but the concept needs some further work. Due to the compact structure, the tailless aircraft can be transported without foldable elements, what improves the reliability of the aircraft. The aerodynamic characteristics need to be validated by more advanced software and the high angles of attack need to be also analysed to make sure that aircraft can be also released during the atmospheric entry.

Further Work

The problem of the lateral and directional stability will be analysed in a next step and improving the damping ratio in case of the short period oscillation is also required.

References

Anyoji M, Okamoto M, Fujita K, Nagai H, Oyama A, (2017), "Evaluation of Aerodynamic Performance of Mars Airplane in Scientific Balloon Experiment", Fluid Mechanics Research International Journal Volume 1 Issue 3

Cook, M.V. (2007), Flight Dynamics Principles, Elsevier, Oxford

Etkin, B. and Reid, L.D. (1996), Dynamics of flight. Stability and Control, John Wiley & Sons Inc., New York, NY.

Figat, M.; Galiński, C.; Kwiek, A. (2012). „Modular Aeroplane System. A Concept and Initial Investigation", in Proceedings of ICAS 2012 Conference, 23–28 September 2012, Brisbane, Australia.

Galiński, C.; Goetzendorf-Grabowski, T.; Mieszalski, D. Stefanek, Ł. (2007). „A concept of two-staged spaceplane for suborbital tourism", Transactions of the Institute of Aviation 191(4) pp.33–42.

Goetzendorf-Grabowski T., Mieszalski D.,Marcinkiewicz E., (2011), "Stability analysis using SDSA tool, Progress in Aerospace Sciences", Vol. 47, Issue 8, November, pp. 636-646

Guynn M. D., Croom M. A., Smith S. C., Parks R.W, Gelhausen P.A., (2003)"Evolution of a Mars Airplane Concept for the ARES Mars Scout Mission", 2nd AIAA "Unmanned Unlimited" Systems, Technologies, and Operations — Aerospace15 - 18 September 2003, San Diego, California, AIAA 2003-6578

Justus, C. G., Johnson, D. L., (2001), "Mars Global Reference Atmospheric Model 2001 Version (Mars-GRAM 2001): Users Guid", NASA Report TM-2001-210961

Kwiek A., Figat M. (2016), "LEX and wing tip plates' interaction on the Rocket Plane in tailless configuration", The Aeronautical Journal Vol. 120, Issue 1224, pp. 255-270

MIL-F-8785C—military specification flying qualities of piloted airplanes, 5 November 1980

NASA website: https://mars.nasa.gov/insight/mission/overview/

Naoya Fujioka, Taku Nonomura, Akira Oyama, Makoto Yamamoto and Kozo Fujii (2014). "Computational Analysis of Aerodynamic Performance of Mars Airplane", Trans. JSASS Aerospace Tech. Japan
Vol. 12, No. ists29, pp. Tk_1-Tk_5, 2014

Nelson, R. (1998), Flight stability and Automatic Control, McGraw-Hill, New York, NY.

Noth, A., Bouabdallah, S., Michaud, S., Siegwart, R. and Engel, W. (2004), “SKY-SAILOR Design of an autonomous solar powered martian airplane” In Proceedings of the 8th ESA Workshop on Advanced Space Technologies for Robotics, (ASTRA 2004), Noordwick, Netherland,2004

Panukl https://www.meil.pw.edu.pl/add/ADD/Teaching/Software/PANUKL, 2018

SDSA https://www.meil.pw.edu.pl/add/ADD/Teaching/Software/SDSA , 2018

Young L. A, Aiken E., Lee P., Briggs G., (2005), "Mars rotorcraft: possibilities, limitations, and implications for human/robotic exploration", 2005 IEEE Aerospace Conference, ISBN: 0-7803-8870-4

Nomenclature

Symbols

b – wingspan [m]

C_D – drag coefficient

C_L – lift coefficient

CM – pitching moment coefficient

DR – damping ratio

g – gravity acceleration [m/s^2]

Iy – moment of inertia respect in a body axis system [kg m^2]

m– mass [kg]

q – angular velocities around y axis [rad/s]

S – reference area [m^2]

T – period [s]

$T_{1/2}$ – time to half damping [s]

Ufreq – undamped frequency

δe – elevons (elevator) deflection [deg.]

Definitions, Acronyms and Abbreviations

MAC – mean aerodynamic chord [m]

SDSA – Simulation and Dynamic Stability Analysis

UAV – Unnamed Aerial Vehicle